IET Circuits, Devices & Systems

Research Article

IET Journals
The Institution of Engineering and Technology

NeuroMonitor: a low-power, wireless, wearable EEG device with DRL-less AFE

ISSN 1751-858X
Received on 5th July 2016
Revised 8th February 2017
Accepted on 10th March 2017
doi: 10.1049/iet-cds.2016.0256
www.ietdl.org

Sergi Consul-Pacareu[1], Ruhi Mahajan[1], Mohammad J. Abu-Saude[1], Bashir I. Morshed[1] ✉

[1]*Electrical and Computer Engineering Department, The University of Memphis, Memphis, TN 38152, USA*

✉ *E-mail: bmorshed@memphis.edu*

Abstract: Electroencephalography (EEG) is an effective tool to non-invasively capture brain responses. Traditional EEG analogue front end (AFE) requires a driven right leg (DRL) circuit that restricts the number of channels of the device. The authors are proposing a new 'DRL-less' AFE design, and have developed a wearable EEG device (NeuroMonitor), which is small, low-power, wireless, and battery operated. The EEG device with two independent channels was fabricated on an 11.35 cm^2 PCB that contained a system-on-a-chip microcontroller, a low-noise instrument amplifier, a low-power Bluetooth module, a microSD, a microUSB, and a LiPo battery. The DRL circuit was eliminated by utilising the high CMRR instrument amplifier with differential inputs, and followed by a modified high-Q active Twin-T notch filter (($f_c^{Notch} = 60$ Hz, -38 dB). The signal was conditioned with a band-pass filter composed of a two-stage 2nd-order Chebyshev-I Sallen-Key low-pass filter cascaded with a passive 2nd-order low-pass filter ($f_c^{LP} = 125$ Hz) and a 1st-order passive high-pass filter ($f_c^{HP} = 0.5$ Hz). Finally, the signal was amplified to achieve an overall gain of 55.84 dB, and digitised with a 16-bit delta-sigma ADC (256 sps). The prototype weighs 41.8 gm, and has been validated against a research-grade EEG system (Neuroscan).

1 Introduction

Naturalistic environment monitoring of brain response is a critical next-generation cyber physical systems for brain computer interfacing (BCI) that can be realised with wearable or body-worn embedded systems (ES) [1–3]. Wearable ambulatory systems to unobtrusively capture neuro-physiological signals at natural settings has the potential to transform the traditional monitoring of neurological disorder patients that can have significant impact on diagnosis, prognosis, therapy, and rehabilitation of neurological disorder patients [4–8].

Commonly utilised non-invasive neuro-signal recording techniques include electroencephalography (EEG), magnetoencephalography (MEG), positron emission tomography (PET), and functional magnetic resonance imaging (fMRI), and functional near infra red (fNIR) [2, 9]. Among these techniques, EEG and MEG have excellent temporal resolution, while PET, MEG and fMRI have higher spatial resolution. EEG and MEG are direct brain signal recordings, as EEG captures electric activities of neuronal firing through conductive coupling, and MEG captures magnetic signals generated from neuronal firing. In contrast, fMRI and fNIR are indirect measures of neuronal activities through blood-oxygen-level dependent (BOLD) technique [1]. MEG, fMRI and PET require highly sensitive magnetic sensors (e.g. superconducting material-based SQUID [10]) enclosed inside a large, heavy, and expensive equipment, and usually confined within a magnetically shielded room (MSR); hence they are not suitable for monitoring patients outside of clinical settings [1]. EEG sensors, on the contrary, are miniature, lightweight, and low-cost. Furthermore, it can be conveniently worn for continuous sensing beyond clinical settings for continuous brain signal monitoring [1, 9, 11].

Many devices currently exist with capability to capture EEG data with a wearable device and transmits data wirelessly in real-time. The 14-channel EPOC and Insight neuro-headsets (from Emotiv) connect wirelessly to a computer using USB receivers, and can provide access to raw EEG data for 12 h. B-Alert X4 has a 4-channel EEG system with online and offline storage capability, and can be attached to the head with a harness. The first FDA-approved single-channel EEG recording device iBrain is also small and portable. Other examples of single channel EEG system are MindWave, ThinkGear and MindSet from NeuroSky. Furthermore, many research articles have presented various types of EEG systems and sensors including ModularEEG from OpenEEG project and OpenBCI from OpenBCI project [4, 12–15]. Besides, various wireless EEG based medical devices have been demonstrated for effective data collection and analysis [14–17].

In the traditional design approach, driven right leg (DRL) circuit is utilised to reject the common mode noise by injecting amplified noise to cancel the interference. This DRL circuit design constrains modularity and scalability for EEG channels due to interdependency of channels, as the number of channels of the system needs to be fixed at the design time for optimal operation. In fact, DRL circuit might increase differential mode noise if not properly matched [18]. This restricts the number of channels for the EEG system at deployment time. In this paper, we present a new design of the analogue front end (AFE) with a unipolar battery-operated, small, low-power, wearable ambulatory EEG data collection device, referred herein as 'NeuroMonitor'. We achieved the independent channel design of EEG device by eliminating the DRL circuit using our new AFE, and replacing DRL electrode with the reference (mid-rail) of the circuit [19–24]. DRL-less EEG systems can be designed for each channel independently without any reliance of the total number of EEG channels to be deployed.

2 System model

2.1 System configuration

We have designed a new modular unipolar AFE circuit design powered by a small rechargeable battery of Lithium-polymer (LiPoly or LiPo) type. Fig. 1 shows the overview of NeuroMonitor device block diagram to wirelessly collect EEG data from the ambulatory NeuroMonitor device. The NeuroMonitor hardware consists of two independent channels of AFE. The AFE schematic of each channel of the NeuroMonitor device is given in Fig. 2.

One of the critical issues for modular and scalable design of EEG system is that the standard configuration requires a feedback of amplified noise to the body of all the channels to cancel the interference, commonly known as DRL circuit, a concept originated from early bioelectronics experiments of bio-potentials such as ECG [25]. The prime rationale of DRL as outlined in the pioneering paper [25] is to eliminate (i) dangerous current flow through the ground loop and (ii) large voltage build up on patient

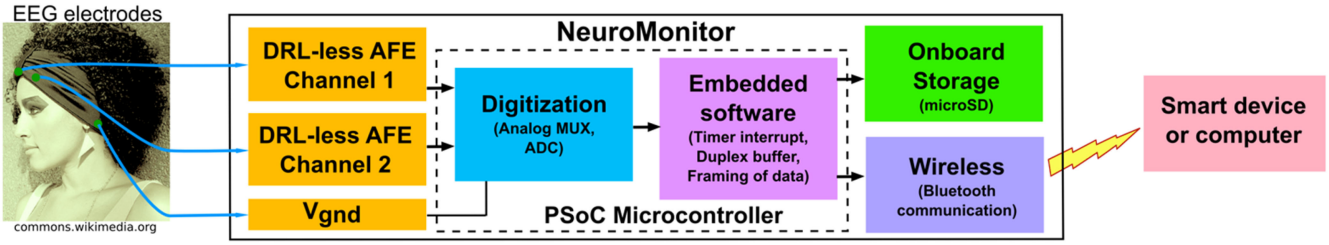

Fig. 1 *Block diagram depicting the key elements of the prototyped DRL-less EEG device (NeuroMonitor) with two independent channels (attached to FP1 and FP2 locations) and communicating wirelessly with a smart device*

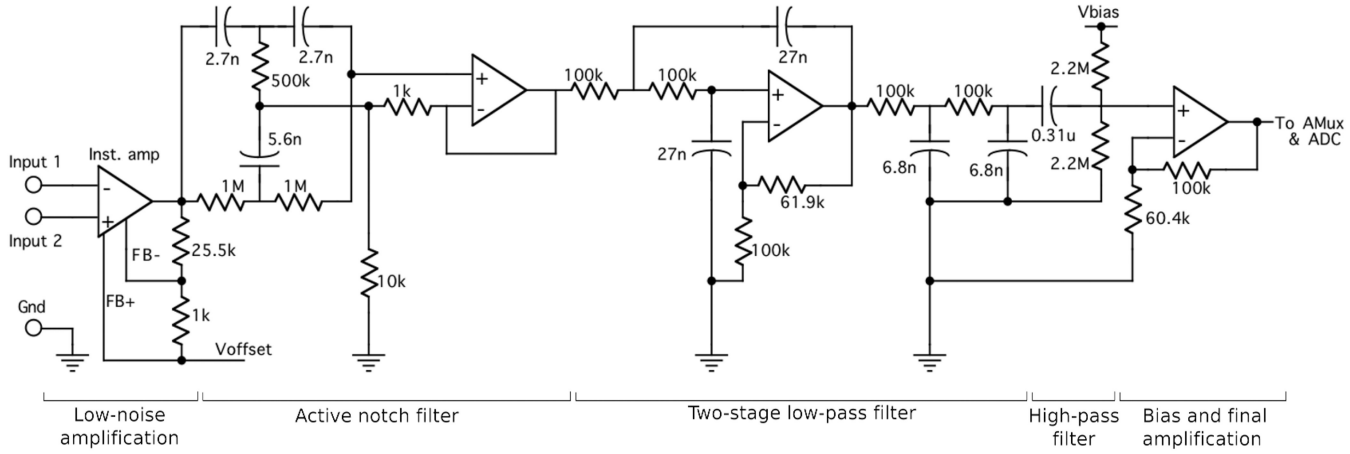

Fig. 2 *Schematic diagram of the proposed AFE design for each independent channel of EEG data for the NeuroMonitor device*

across a poorly connected electrode. These issues are not applicable for new generation of battery-operated EEG devices that are fully disconnected from the wall power supply. Further noting that for battery operated fully wireless ambulatory devices, the stray capacitance between the amplifier common and earth ground, C_s, is significantly smaller that for wall power devices, hence i_{d2} as given in (1) of [25] becomes negligible. This drastically reduces v_c leading to invalidating the motive of DRL circuit to minimise v_c (Fig. 3 of [25]). In addition, DRL circuit might increase differential mode noise if not properly matched, which is a severe design barrier for modular and scalable EEG systems [18]. Nonetheless, DRL based design even for battery operated EEG systems are still utilised [6, 10–12, 14]. Elimination of DRL will allow development of independent channel of EEG nodes towards a reconfigurable and saleable system, which can incorporate other types of sensors (e.g. breathing rate) within the network [26].

Instead of conventional approach to reduce interfering noise using DRL, we have employed differential amplifier followed by a notch filter configuration that minimises the power line interference. Noise and artefact in EEG system is significant as the EEG signal amplitudes of interest are only within 100 μV range. The $1/f$ noise is dominating at low frequencies and can contaminate the signals significantly. At higher frequencies, white noise will be dominating after the $1/f$ corner frequency. However, for a practical system, power line interference noise (60 Hz for USA) is far more significant and within the bandwidth of the signal of interest. We utilised a high-Q notch filter to reduce this within acceptable range.

SNR is defined as $\mathrm{SNR(db)} = 10\log(P_{\mathrm{sig}}/P_{\mathrm{noise}})$, where P_{sig} and P_{noise} are the power of the signal and noise respectively. Noise figure (NF) is defined as $\mathrm{NF} = (\mathrm{SNR_i}/\mathrm{SNR_o})$, where $\mathrm{SNR_i}$ is the noise in the input signal and $\mathrm{SNR_o}$ is the noise in the output signal. If the noise in the input signal is N_s, the gain of the amplifier stage is G, and the noise introduced by the amplifier is $N_{\mathrm{amp,o}}$, then:

$$\mathrm{NF} = \frac{(P_{\mathrm{sig}}/N_s)}{(GP_{\mathrm{sig}}/(GN_s + N_{\mathrm{amp,o}}))} = \frac{N_s + (N_{\mathrm{amp,o}}/G)}{N_s} = 1 + \frac{N_{\mathrm{amp,i}}}{N_s} \geq 1 \quad (1)$$

Here, $N_{\mathrm{amp,i}} = N_{\mathrm{amp,o}}/G$ is called input referred noise. Due to this noise, any stage of a cascaded amplifier will be exposed to additional noise as given in (1). Hence noise suppression is more effective at an earlier stage. For instance, in a two stage cascaded system, denoted by subscripts 1 and 2 respectively, it can be shown that the overall NF is [27]

$$\mathrm{NF_{overall}} = 1 + \frac{N_s(NF_1 - 1) + (N_s(NF_2 - 1)/G_1)}{N_s} = NF_1 + \frac{NF_2 - 1}{G_1} \quad (2)$$

Thus, improving $\mathrm{NF_1}$ is more effective than improving $\mathrm{NF_2}$ by a factor of G_1. Thus, we have utilised a very low noise instrument amplifier ($\mathrm{NF_1}$), and suppressed noise immediately after that with the notch filter ($\mathrm{NF_2}$).

To protect against baseline wondering and to minimise circuit complexity, we employed a signal-biasing stage (composed of a pair of 2.5 MΩ voltage dividers) after the high-pass filter and just prior to the final amplification stage that prevents output signal from baseline wondering and ensures the baseline of ADC midrange. Some spectral distortions occur due to the notch and pass filters, which can be later improved by fine-tuning the design parameters in subsequent revisions.

The NeuroMonitor AFE design (Fig. 2) composes of two differential inputs, and the ground of the battery is used as the common terminal. The two inputs can be configured in either referential or bipolar montages. For referential montage, Input 2 can be used as the ear mastoid reference. Moreover with bipolar montage, common average referencing can be used to convert it to referential montage. The AFE requires a ground electrode to be connected, which can be at the opposite mastoid behind ear or at central electrode positions (e.g. *Cz*). For bipolar montages, either transverse or longitudinal type can be used.

2.2 Wearable embedded system considerations

Size and weight of the wearable device are major constraints for unobtrusive deployment in a naturalistic setting. Unobtrusive wearable devices can minimise social and personal dogma.

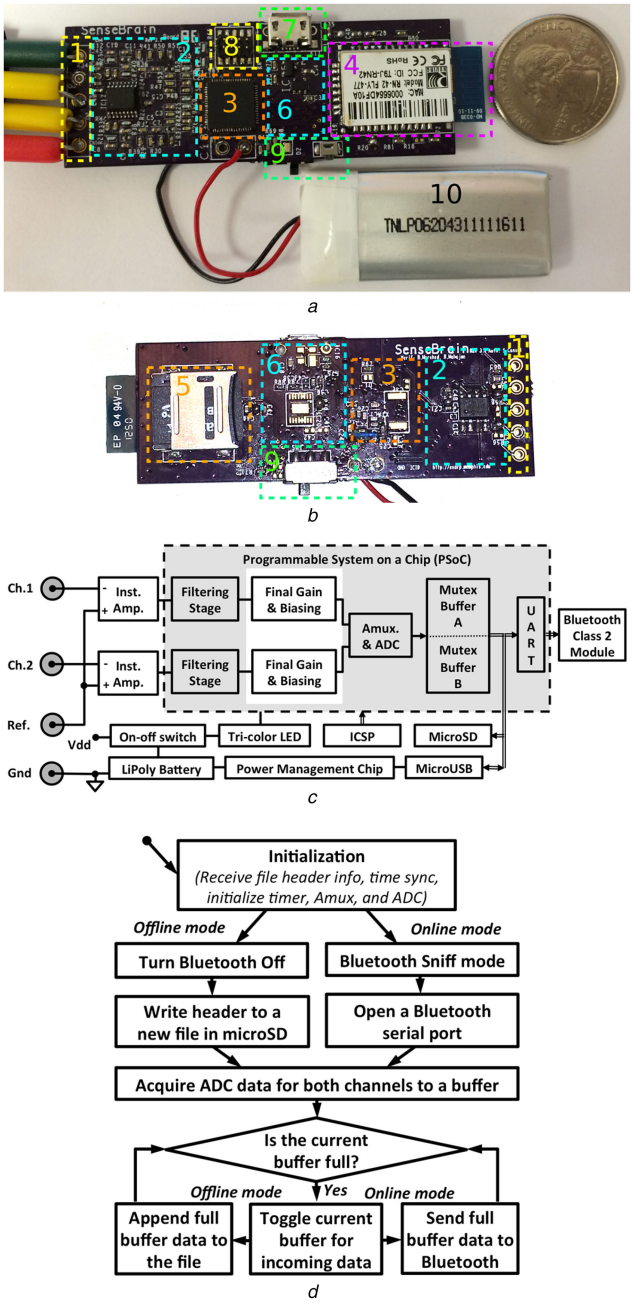

Fig. 3 *(a-b) Photographs of the prototyped NeuroMonitor hardware (55.8 mm × 20.3 mm)*

(a) Top side of the hardware connected to a rechargeable LiPo battery beside a USA quarter, ***(b)*** Bottom side of the hardware. Legends: (1) EEG sensor terminals, (2) AFE, (3) PSoC microcontroller, (4) BT module, (5) microSD card memory, (6) power management circuitry, (7) micro-USB port, (8) ICSP programming port, (9) switches and LEDs, and (10) LiPoly battery, ***(c)*** The functional hardware block diagram of referential montage setup of the NeuroMonitor device. The 2 independent channels of EEG data are spatially separated (in two AFE paths) in the analogue domain, while time-slot separated (not shown) in the digital domain, ***(d)*** The firmware StateChart of the ambulatory NeuroMonitor device for online and offline modes

Furthermore, we restricted our development based on only commercial off-the-shelf components to minimise deployment time and expense. As rechargeable batteries are more practical for daily usage on a wearable device, our primary choices for batteries were among Ni-Cad, Li-Ion and LiPoly, of which LiPoly was selected due to superior energy density, low-profile enclosure and flexibility. Hence, the device operating voltage is set to 3.7 V, nominal voltage of LiPoly battery.

2.3 Online data capture constraints

Online data transmission with industry standard wireless protocols requires special timing guarantees, as the involved processes are asynchronous. For instance, for a sampling rate of 256 sps, the ADC interrupt triggers every 3.9 ms. The sampled data from the ADC needs to be placed in the buffer that maintains this constraint to safeguard against data loss. This is guaranteed by a timer driven interrupt service routine (ISR) approach. The ISR triggers every 3.9 ms will fetch the data from the ADC move it to the buffer. As the time required for the sampled data to transfer to the Bluetooth (BT) through universal asynchronous receiver transmitter (UART) or to append to a file in the microSD memory card is larger than 3.9 ms, a software buffer (memory) with mailbox semaphore was used to minimise memory usage. We have implemented a mutex-buffer pair to sufficiently resolve the timing issue. If the buffer is full, the active buffer is toggled and the full buffer data is either sent to the BT or written to the microSD card depending on the mode selection.

To guarantee against buffer overflow, the time required for transmission of each buffer data must satisfy this constraint

$$T_{\text{trans}} < T_{\text{buf}} = \frac{T_{\text{samp}} \times S_{\text{buf}}}{N_{\text{ch}} \times S_{\text{samp}}} \tag{3}$$

where T_{trans} is the time required to transmit a full buffer, T_{buf} is the time required to fill up a buffer, T_{samp} is the sampling period, S_{buf} is the size of buffer in Bytes, N_{ch} is the number of channels that are simultaneously sampled, and S_{samp} (=number of ADC bits / 8) is the digitised data size for each sample in Bytes. The timing guarantee of the buffer was maintained by designing a buffer of large enough size to satisfy the constraint (3), as all other parameters were known.

However, the guarantee of continuous wireless transmission was more challenging due to its inherent of best effort nature, rather than guaranteed transmission when the distance between the transmitter and receiver is out of range. This can cause packet loss or delay in transmission, and can ultimately have discontinuity in received data. This is critical when EEG data is analysed, as erroneous feature or classification can stem for discontinuous data. As there is no practical way of such guarantee of continuation, we developed an ad-hoc protocol to detect such discontinuation of wireless transmission by incorporating a serial number for each transmitted buffer packet, and ensuring reception of sequential packets; otherwise flag it as a discontinuity at that point so data can be stored in SD card to minimise data loss.

2.4 Institutional review board (IRB) considerations

As the device was studied with human subjects, an IRB approval was required and obtained using standard procedure. The IRB rules consider the device safety, usage, protocol, recruitment, and consents. The IRB was approved through The University of Memphis IRB committee (Approval Number: 2289).

3 Embedded hardware components

3.1 EEG sensors

EEG sensors convert ionic currents from compounded neuronal firing to electronic currents. These bio-potentials at the scalp are of µV ranges and can be captured with wet or dry type Ag/AgCl electrodes [9]. We have used a commercial disposable adhesive pre-gelled electrode (GS-26, Bio-Medical Instruments, Warren, MI) suitable for EEG data collection from the prefrontal cortex. The sensor contains a 0.5% saline base gel on a 10 mm flat pellet Ag/AgCl electrode surrounded by a paper-thin transparent self-adhesive tape disc of 1-inch diameter.

EEG signals are typically classified as delta (0.1–3.5 Hz), theta (4–7.5 Hz), alpha (8–13 Hz), beta (14–30 Hz), and gamma (>30 Hz) rhythms. We have designed the AFE to capture signals within the range of 0.5 to 125 Hz. Our design constraint was set for a unipolar supply. EEG signals at scalp are roughly less than 100 µV

Table 1 AFE parameters of different stages

Stage	Implementation	Gain	Cutoff
low-noise amplification	differential instrument amplifier	26.5	—
notch filter	active band stop	1	60 Hz
LPF	two-stage 2nd order Sallen Key active cascaded to 2nd order passive	1.61	125 Hz
HPF	one-stage passive filter	0.83	0.5 Hz
gain	non-inverting amplifier	17.5	—

and 100 Hz, which require extremely low-noise differential mode amplification and high input impedance amplifier.

A unipolar differential amplifier (ISL28270, Intersil Americas, Palm Bay, FL) with 110 dB CMMR and rail-to-rail input and output (RRIO) was used as the first stage (Fig. 2). Note that newer models of unipolar instrument amplifier can be used with possible improvement of performance. To allow full signal swing without clipping, a bias of 1.024 V was supplied to the instrument amplifier from the DAC of the microcontroller. The differential amplifier is followed by a modified active Twin-T notch filter ($f_c^{\text{Notch}} = 60$ Hz, −38 dB) implemented with an op-amp that reduces power line interference, which is the dominating noise in EEG signals in the absence of the DRL circuit. The signal is then passed through a band-pass filter composed of a 2nd-order Chebyshev-I low-pass Sallen-Key filter cascaded with a 2nd-order low-pass filter ($f_c^{\text{LP}} =$ 125 Hz) followed by a 1st order high-pass filter ($f_c^{\text{HP}} = 0.5$ Hz). It should be noted that the notch and other filters might cause spectral distortion, which may reach the signal band. We utilised two internal op-amps of the PSoC3 microcontroller chip (CY8C3866-030LTI, Cypress Semiconductor Corp., San Jose, CA). Signal is then biased at mid-rail, and passed through a final amplification stage to achieve a total of 55.84 dB ($A_v = 619.7$) amplification with an op-amp (MCP6002, Microchip Technologies Inc., Chandler, AZ). This analogue signal is then sampled with an analogue mux and ADC of the PSoC3 chip. The specifications of the AFE are tabulated in Table 1.

3.2 Signal digitisation

The NeuroMonitor prototype was developed to capture two EEG channels simultaneously. Two independent AFE were designed on a 4-layer PCB using Cadence Allegro software (Cadence Design Systems Inc., San Jose, CA, USA). The analogue mux is triggered by a timer interrupt to sample the signals of the two channels in sequence at 256 sps, and digitise the analogue signal with a delta-sigma 16-bit ADC, which is built into the PSoC3 chip. Photographs of the prototype, hardware block diagram, and firmware StateChart are depicted in Fig. 3.

3.3 Microcontroller

The microcontroller (PSoC3) contains reconfigurable hardware including op-amps, DSP modules, ADCs and DACs, etc. The PSoC3 can operate at 62-MHz clock with 3.3 V supply. It contains a single cycle 8051 CPU core, flash memory of 64 KB, 8 KB of SRAM, and 2 KB of EEPROM. It also contains a 24-channel direct memory access (DMA), and SPI, UART, I^2C, and USB 2.0 ports. Firmware of the microcontroller was developed with PSOC Creator, and programmed to the microcontroller with MiniProg3 JTAG programmer through ICSP port.

3.4 Wireless communication

The NeuroMonitor contained a wireless BT interfacing module (RN-42, Roving Networks, Los Gatos, CA). This is a Class 2 module with BT 2.1 stack. The hardware is 13.4 mm × 25.8 mm × 2 mm. The module has integrated folded PCB antenna for 2.4 GHz ISM band. It is extremely low power BT module (26 μA sleep, 3 mA connected, and 30 mA transmit). It allows UART communication in Serial Port Profile (SPP) mode. The transmission range of the BT module can cover up to 20 m. The baud-rate for transmission is set to be 115.2 kbps. To reduce power consumption, we used sniff mode at 100 ms interval for 5 ms.

3.5 Power management and other peripherals

A LiPoly battery of 800 mAh was used as the power supply. To ensure that the battery is not overcharged, the charging is controlled by a linear charge management controller (MCP73831, Microchip Technology, AZ, USA). The battery allows continuous collection of EEG data from the two channels for approximately 10 h without any power optimisation as discussed in a later section.

For battery operated wearable devices like NeuroMonitor, the wireless module consumes the highest power, followed by the microcontroller for signal processing [7]. We showed that, except AFE, other stages could be switched to low power mode to optimise power consumption [20]. The total power consumption of the device can be represented as:

$$\begin{aligned} P_{\text{Total}} &= P_{\text{ADE}} + P_{\text{Digitize}} + P_{\text{DBE}} + P_{\text{St}} + P_{\text{Trans}} \\ \Rightarrow P_{\text{Total}} &= P_{\text{ADE}} + (D_{\text{On}} \times P_{Digitize\_on} + D_{\text{Off}} \times P_{Digitize\_off}) \\ &\quad + (D_{\text{On}} \times P_{DBE\_on} + D_{\text{Off}} \times P_{DBE\_off}) \\ &\quad + (S_{\text{On}} \times P_{St\_on} + S_{\text{Off}} \times P_{St\_off}) \\ &\quad + (T_{\text{On}} \times P_{Trans\_on} + T_{\text{Off}} \times P_{Trans\_off}) \end{aligned} \tag{4}$$

where P_{Total} is the average total power consumed over a long period, and D_{on} is the fraction of time the ADC and DBE blocks are ON, while D_{off} is the corresponding fraction of OFF period. Similarly, S_{on} and T_{on} are the fraction of time the storage and transmission modules are ON, respectively, and S_{off} and T_{off} are the corresponding fraction of OFF period.

The 4-layer PCBs were fabricated by OSH Park (www.oshpark.com). The populations of the boards were done with air reflow workstation (SMD rework station 858D). Most passive SMD components were selected from smaller profiles (e.g. 0402 footprints for registers) to reduce footprint.

4 Embedded firmware implementation

4.1 Configuration and initialisation

The NeuroMonitor system operates in two data collection modes: online mode and offline mode. These modes can potentially be selected to dynamically assign based on the availability of neighbouring wireless reception unit for online mode. In the online mode, data is streamed in real-time to a wireless remote computing system for data reception. In the offline mode, data is stored in the onboard non-volatile memory such as microSD card or Flash memory chip.

4.2 Data acquisition

A timer is initialised to trigger at 3.9 ms to collect ADC data. The ADC data is placed into the buffer using ISR. The size of each mutex buffer is set to 512 Bytes, which satisfies the constraint (3) in addition to reducing power consumption utilising sniff mode of the BT. The ISR also checks for buffer full. Based on the initialisation of online or offline mode, the data flows with different paths as shown in Fig. 3*d*. If offline mode is selected, the data is appended to a data file in the microSD card. However, this process does not allow for online monitoring of the data. The online mode, on the contrary, data is transmitted through the BT port and can be monitored in real time to ensure proper data collection.

5 Software interface implementation

The mode selection can be performed at the beginning of the session with a graphical user interfacing (GUI) developed with Visual Basic.Net (ver. 2010, Microsoft Corp., WA, USA). The

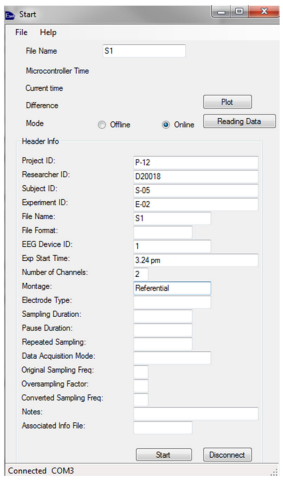

a

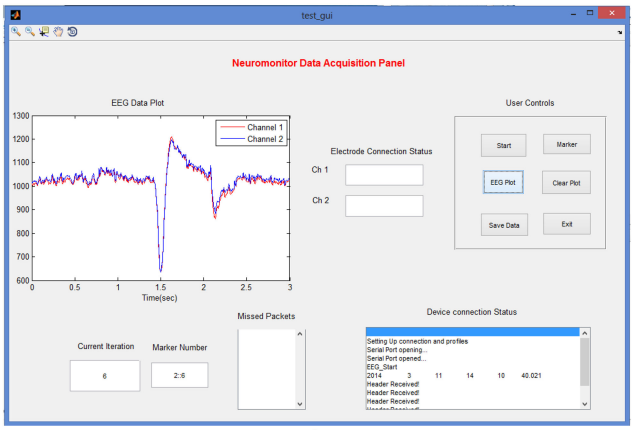

b

Fig. 4 *Initialisation interface also allows for metadata association such as date, time, patient ID, study ID, session number, and custom file name*
(a) Setup/Initialisation interface, ***(b)*** Online data capture interface showing an eye blink artifact at 1.5 s

initialisation interface also allows for metadata association such as date, time, patient ID, study ID, session number, and custom file name (Fig. 4*a*). The interfacing GUI can communicate with the NeuroMonitor using the USB port or the BT port. A GUI panel was also developed with Matlab (Mathworks Inc., MA, USA) to collect and store data in remote computer for online mode (Fig. 4*b*). This GUI also has provision to monitor if data packets are not in sequence. It also monitors if the EEG data is beyond limit, which might be due to the electrodes not properly positioned or becoming loose. The GUI further allows inserting of trigger markers for different activities, which allows synchronisation of EEG data with the corresponding events, which are manually written down in the activity log.

6 Functional testing and verification

6.1 Bench testing results and power optimisation

The recorded data has been captured and analysed with Matlab (Mathworks Inc., MA, USA) and EEGLAB. The EEG data is correlated with blinks and validated against a commercial system as discussed here [21]. Even though the NeuroMonitor prototype could operate for 10 h of continuous monitoring, we investigated dynamic clock frequency shifting (DFS) technique to further optimise power [20]. The optimisation has resulted in a five-fold improvement with 12 MHz clock at operating frequency (step-up) and 3 MHz during idling period (nominal) (Fig. 5). The current consumption for instrument amplifier, opamp, and filter-stages were 217, 400, and 300 µA, respectively [20]. The BT module consumes the most power, hence the power optimisation was achieved by using 100 ms sniff mode.

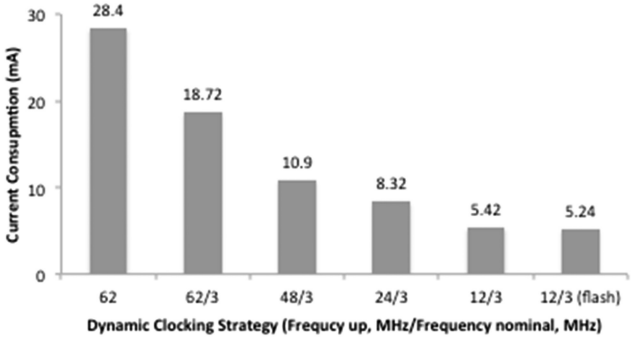

Fig. 5 *Power consumption optimisations of the device with DFS technique*

6.2 Raw EEG data and artefact removal

Eye-blink artefacts have to be removed from EEG data especially for the prefrontal cortex electrodes (FP1 and FP2), since artefacts (such as eye-blinks) significantly impact EEG data at these sites. We have developed a wavelet enhanced independent component analysis (ICA) algorithm to remove artefacts automatically using Kurtosis and modified multi-scale entropy identification of artefactual components [28, 29]. However, for EEG systems with very few channels, ICA artefact removal is challenging, as the number of independent components are less than the number of input channels. Hence, for system with one or two input channels, ICA cannot be applied. We are investigating a wavelet-based hardware-efficient approach for single channel online eye-blink artefact removal to be implemented in the NeuroMonitor [30]. Wavelet based method is one of the very promising methods for artefact removal from single channel EEG system, as wavelet transform only requires single channel data.

6.3 Analysis and comparison of data

To validate the EEG data collection of the NeuroMonitor device, we have compared the data with a research-grade 64 mono-polar channel EEG system (Neuroscan SynAmps RT, Compumedics Neuroscan USA, Ltd. Charlotte, NC, USA). The controlled data was collected in a MSR. The data were collected from paired electrodes (one connected to NeuroMonitor, and the other connected to Neuroscan) at minimal gaps that is achievable within practical constrain. A representative time-frequency spectrograph is shown in Fig. 6. The data from both devices correlated well in both time and frequency domain. For instance, FP1 data for NeuroMonitor and Neuroscan had correlation coefficients for blink and non-blink periods of 0.8813 and 0.766, respectively [21]. Other statistics such as Kurtosis showed similarity too (17.68 and 19.45 for blink and 1.125 and 0.8075 for non-blink, respectively). Power spectral density (PSD) waveforms also correlated well. Fig. 7 shows temporal raw EEG data from FP1 and FP2 for these two devices, which depict a good agreement of data. In regards to an in-depth analysis of noise comparison of this ‘DRL-less’ design in comparison to traditional DRL-based designs, enthusiastic readers can refer to our related publication [31].

7 Evaluation through deployment

The artefact removed EEG data can be applied for various feature extraction and classification of brain activities. The advantage of NeuroMonitor being a small and portable device is that the data can be collected unobtrusively at naturalistic environment, a grand challenge for the BRAIN Initiative [1].

We have performed multiple pilot study sessions with the NeuroMonitor device [19, 22, 29]. In one of the study, the subjects were asked to perform three different cognitive tasks:

- *Math:* Solve challenging mathematical quizzes.
- *Music:* Enjoy soothing music with eyes closed.
- *Game:* Play an engaging game (snake dots).

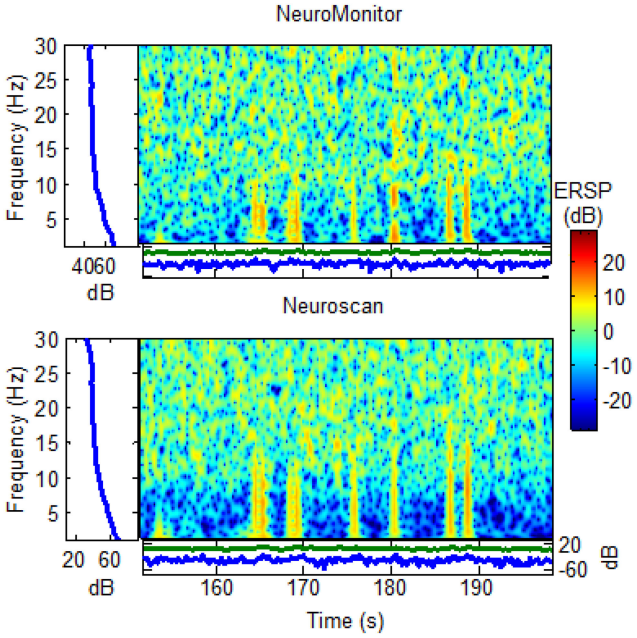

Fig. 6 *Time-frequency spectrograph of data collected from FP1 with the NeuroMonitor device, in comparison to Neuroscan commercial EEG system*

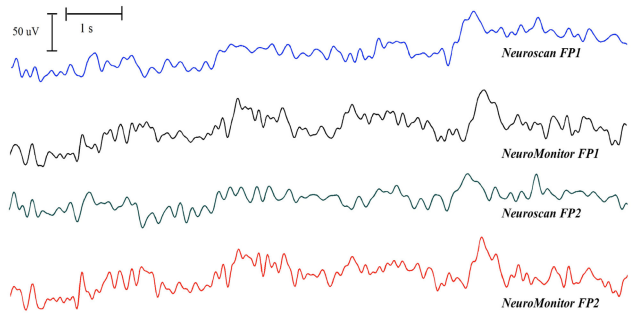

Fig. 7 *Comparison of the captured EEG data with NeuroMonitor device and a commercially available clinically approved Neuroscan system for (approximately) the same scalp locations (FP1 and FP2)*

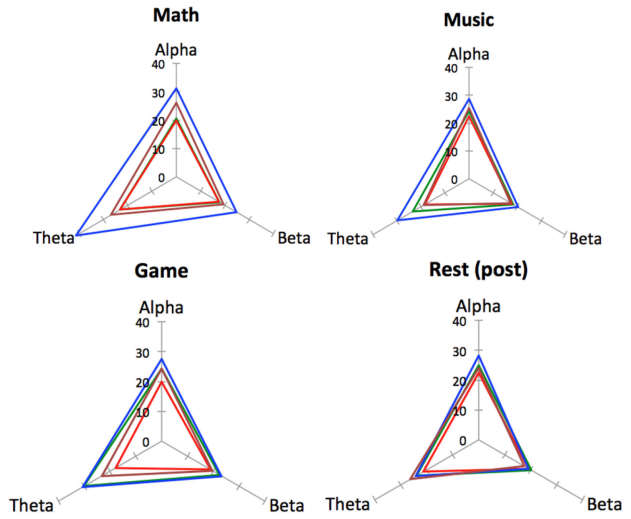

Fig. 8 *Engagement study results for four subjects (indicated with four different colours in the plots) performing Math, Music, Game, and Rest (post) tasks in various sessions. The data shows the ability of NeuroMonitor EEG device to capture variations of rhythm powers (PSD) for Alpha, Beta, and Theta bands with different activities, which can be utilised for real-time activity classification*

Baseline data were collected from pre- and post-rest sessions. The device was configured for two channel referential montage with online mode. PSD of Alpha (8–13 Hz), Beta (13–30 Hz), and Theta (4–8 Hz) rhythms from FP2 location are plotted in Fig. 8 for four subjects (denoted with different colours). Analysis of these data shows that the brain engagement or cognitive activity levels for *Math* and *Games* were higher compared with other sessions. Moreover it depicts significant variation of results among different subjects, since no two people are identical in terms of brain activities. From the study shown here, and other related study reported elsewhere [19, 21–24], the functionality and usability of the small and wearable NeuroMonitor device has been demonstrated for neuro-physiological data acquisition and applications.

Along with these controlled studies, NeuroMonitor device was also deployed to collect brain activity data at a classroom setting to monitor engagement of children (2–3 years) [22]. These studies show promise to study brain activities of patients such as Autism Spectrum Disorder, or cerebral palsy, in natural environment. Brain activity monitoring of patients with neurological disorders (such as symptomatic or cryptogenic epilepsy) will significantly enhance efficacy of patient care. Similar monitoring can be beneficial to Alzheimer's, post-traumatic stress disorder, and attention deficit hyperactivity disorder patients, as well as for assessment of working memory load and cognitive stress by detecting corresponding events of interests.

8 Conclusions

This paper presents a wireless ambulatory EEG data collection device (NeuroMonitor) for 2-channel referential or bipolar montage with 'DRL-less' AFE. Elimination of DRL further simplifies the design, and reduces power requirement for DRL circuitry, allowing for a truly reconfigurable independent channel EEG systems [26]. This DRL-less system for battery powered wearable devices, such as ECG and EEG, will reduce AFE complexity and allow modular design. The prototyped device dimension is 2.2″ × 0.8″ × 0.36″, weighs only 41.8 gm, operates on a LiPoly battery, communicates wirelessly with BT enabled device, and can be completely concealed within wearable accessories suitable for brain activity monitoring at natural settings. At this prototyping stage, the cost per unit was less than $50 USD. The use of unipolar power supply reduces battery constraint. The use of the battery allows eliminations of DRL, which allows independent channel design for EEG system. This was achieved by utilising a very low-noise, high CMRR instrument amplifier followed by a high-Q active notch filter to suppress the common mode noise. The device consumes only 5.24 mA leveraged with DFS technique. Besides being small size, lightweight, low-power, wireless, and requiring only unipolar power supply, a unique feature of NeuroMonitor is the elimination of DRL circuit towards modular and scalable EEG system [26]. The validation and deployment provides evidence that such a wearable ambulatory EEG devices can be applied for studies related to brain activity monitoring in real-life settings and neurological patient diagnosis and rehabilitation beyond clinical settings, cognitive load assessment in work environment, and psychological studies related to collaborative learning, shared intention and social interaction.

9 Acknowledgments

This work was partly supported by Strengthening Communities Initiative – Capacity Building Grant (2012-CB1) and FedEx Institute of Technology Innovation Grant (grant no. 2013-537908) of The University of Memphis.

10 References

[1] He, B., Coleman, T., Genin, G.M., *et al.*: 'Grand challenges in mapping the human brain: NSF workshop report', *IEEE Trans. Biomed. Eng.*, 2013, **60**, (11), pp. 2983–2992

[2] Zheng, Y., Ding, X., Poon, C.C.Y., *et al.*: 'Unobtrusive sensing and wearable devices for health informatics', *IEEE Trans. Biomed. Eng.*., 2014, **61**, (5), pp. 1538–1554

[3] Alemdar, H., Ersoy, C.: 'Wireless sensor networks for healthcare: a survey', *Comput. Netw.*, 2010, **54**, pp. 2688–2710

[4] Lin, R., Lee, R., Tseng, C., *et al.*: 'Design and implementation of wireless multi-channel EEG recording system and study of EEG clustering method', *Biomed Eng. Appl. Basis Commun.*, 2006, **18**, (6), pp. 276–283

[5] Tapia, M., Intille, S., Lopez, L., *et al.*: 'The design of a portable kit of wireless sensors for naturalistic data collection'. Proc. Intl. Conf. Pervasive Comp, 2006, pp. 117–134
[6] Casson, A.J., Yates, D.C., Smith, S.J.M., *et al.*: 'Wearable Electroencaphalography', *IEEE Eng. Med. Biol. Mag.*, 2010, pp. 44–57
[7] Patel, S., Park, H., Bonato, P., *et al.*: 'A review of wearable sensors and systems with application in rehabilitation', *J. Neuroeng. Rehabil.*, 2012, **9**, (21), pp. 1–17
[8] Morshed, B.I., Massa, A.: 'Cutting-edge technology for a cognitive load performance assessment system', *MEDS Mag.*, 2013, pp. 16–18
[9] Morshed, B.I., Khan, A.: 'A brief review of technologies and challenges to monitor brain activities', *J. Bioeng. Biomed. Sci.*, 2014, **4**, (1), pp. 1–10
[10] Chi, Y.M., Jung, T., Cauwenberghs, G.: 'Dry-contact and noncontact biopotential electrodes: methodological review', *IEEE Rev. Biomed. Eng. Front. Neurosci.*, 2010, **3**, pp. 106–119
[11] Lin, C., Ko, L., Chiou, J., *et al.*: 'Noninvasive neural prosthesis using mobile and wireless EEG', *Proc. IEEE*, 2008, **96**, (7), pp. 1167–1183
[12] Zhu, L., Chen, H., Zhang, X., *et al.*: 'Design of portable multi-channel EEG signal acquisition system'. 2nd Intl. Conf. on BioMedical Engineering and Informatics (BMEI), Tianjin, China, October 2009, pp. 1–4
[13] Gnecchi, J.A.G., Lara, L.R.S., Garcia, J.C.H.: 'Design and construction of an EEG data acquisition system for measurement of auditory evoked potentials'. Electronics, Robotics and Automotive Mechanics Conf., Morelos, Mexico, 2008, pp. 547–552
[14] Debener, S., Minow, F., Emkes, R., *et al.*: 'How about taking a low-cost, small, and wireless EEG for a walk?', *Psychophysiology*, 2012, **49**, (11), pp. 1617–1621
[15] Gargiulo, G., Bifulco, P., Calvo, R.A., *et al.*: 'A mobile EEG system with dry electrodes', IEEE Biomedical Circuits and Systems Conf., Baltimore, MD, 2008, pp. 273–276
[16] Schuyler, R., White, A., Staley, K., *et al.*: 'Epileptic seizure detection', *IEEE Eng. Med. Biol. Mag.*, 2007, **26**, (2), pp. 74–81
[17] Lin, C., Ko, L., Chiou, J., *et al.*: 'Noninvasive neural prostheses using mobile and wireless EEG', *Proc. IEEE*, 2008, **96**, (7), pp. 1167–1183
[18] Gomez-Clapers, J., Serrano-Finetti, E., Casanella, R., *et al.*: 'Can driven-right-leg circuits increase interference in ECG amplifiers?'. Annual Intl. Conf. of the IEEE EMBC, 2011, pp. 4780–4783
[19] Mahajan, R., Consul-Pacareu, S., AbuSaude, M.J., *et al.*: 'Ambulatory EEG NeuroMonitor platform for engagement studies of children with development delays'. SPIE Proc. Smart Biomedical and Physiological Sensor Tech X, May 2013, vol. **8719**, p. 87190L(1-10)
[20] Consul-Pacareu, S., Morshed, B.I.: 'Power optimization of NeuroMonitor EEG device: hardware/software co-designed interrupt driven clocking'. 6th Intl. IEEE/EMBS Conf. Neural Engineering, November 2013, pp. 25–28
[21] Mahajan, R., Majmudar, C.A., Khatun, S., *et al.*: 'NeuroMonitor ambulatory EEG device: comparative analysis and its application for cognitive load assessment'. IEEE Healthcare Innovations and Point-of-Care Technologies Conf., Seattle, WA, October 2014, pp. 133–136
[22] Consul-Pacareu, S., Mahajan, R., Sahadat, M.N., *et al.*: 'Wearable ambulatory 2-channel EEG NeuroMonitor platform for real-life engagement monitoring based on brain activities at the prefrontal cortex'. 4th IAJC/ISAM Joint Intl. Conf., FL, September 25–27, 2014, p. 78(1-12)
[23] Sahadat, M.N., Jacobs, E.L., Morshed, B.I.: 'Hardware-efficient robust biometric identification from amplitude and interval features of 0.58 Second Limb (Lead I) ECG signal using logistic regression classifier'. Engineering in Medicine and Biology Society (EMBC), Chicago, IL, August 2014, pp. 1440–1443
[24] Sahadat, M.N., Consul-Pacareu, S., Morshed, B.I.: 'Wireless ambulatory ECG signal capture for cognitive load study using the neuromonitor platform'. 6th Intl. IEEE/EMBS Conf. Neural Engineering, November 2013, pp. 497–500
[25] Winter, B.B., Webster, J.G.: 'Driven-right-leg circuit design', *IEEE Trans. Biomed. Eng.*, 1983, **30**, (1), pp. 62–66
[26] Mahajan, R., Morshed, B.I., Bidelman, G.M.: 'Design and validation of a wearable 'DRL-less' EEG using a novel fully-reconfigurable architecture'. IEEE Engineering Medicine and Biology Society Conf., Orlando, FL, August 16–20, 2016, pp. 4999–5002
[27] Namgoong, W., Lerdworatawee, J.: 'Revisiting the noise figure design metric for digital communication receiver'. Proc. Intl. Symp. Quality Electronic Design, 2003, pp. 159–162
[28] Mahajan, R., Morshed, B.I.: 'Sample entropy enhanced wavelet-ICA denoising technique for eye blink artifact removal from scalp EEG dataset'. 6th Intl. IEEE/EMBS Conf. Neural Engineering, 2013, pp. 1394–1397
[29] Mahajan, R., Morshed, B.I.: 'Unsupervised eye blink artifact denoising of EEG data with modified multiscale sample entropy, kurtosis, and wavelet-ICA', *IEEE J. Biomed. Health Inf.*, 2015, **19**, (1), pp. 158–165
[30] Khatun, S., Mahajan, R., Morshed, B.I.: 'Comparative analysis of wavelet based approaches for reliable removal of ocular artifacts from single channel EEG', 2015 IEEE International Conference on Electro/Information Technology (EIT), Dekalb, IL, 2015, pp. 335–340
[31] Mahajan, R., Morshed, B.I.: 'Performance analysis of a DRL-less AFE for battery-powered wearable EEG measurement', *Meas. J.*, 2016, **90**, pp. 583–591